INVITED PAPER

Long-baseline single-layer 2nd-order high-T_c SQUID gradiometer

Soon-Gul Lee[a,*], Chan Seok Kang[a,b], In-Seon Kim[b] and Sang-Jae Kim[c]

[a] *Korea University, Chungnam, Korea*
[b] *Korea Research Institute of Standards and Science, Daejeon, Korea*
[c] *Cheju National Universit, Cheju, Korea*

긴기저선을 가진 단일층 고온초전도 SQUID 2차미분기

이순걸[a,*], 강찬석[a,b], 김인선[b], 김상재[c]

Abstract

We have studied feasibility of single-layer second-order high-T_c SQUID gradiometers in magnetocardiography. We have measured human cardiomagnetic signals using a short-baseline (5.8 mm) single-layer second-order YBCO gradiometer in partially shielded environments. The gradiometer has an overall size of 17.6 mm × 6 mm and contains three parallel-connected pickup coils which are directly coupled to a step-edge junction SQUID. The gradiometer showed an unshielded gradient noise of 0.84 pT/cm^2/Hz$^{1/2}$ at 1 Hz, which corresponds to an equivalent field noise of 280 fT/Hz$^{1/2}$. The balancing factor was 10^3. Based on the same design rules as the short-baseline devices, we have studied fabrication of 30 mm-long baseline gradiometers. The devices had an overall size of 70.2 mm × 10.6 mm with each pickup coil of 10 mm x 10 mm in outer size. As Josephson elements we made two types of submicron bridges, which are variable thickness bridge (VTB) and constant thickness bridge (CTB), from 3 μm-wide and 300 nm-thick YBCO lines with a thin layer of Au on top by using a focused ion beam (FIB) patterning method. VTB was 300 nm wide, 200 nm thick, 30 nm long with Au removed and CTB 100 nm wide and 30 nm long. In temperature-dependent critical currents, $I_c(T)$, VTB showed an nonmetallic barrier-type behavior and CTB an SNS behavior. We believe that those characteristics are ascribed to naturally formed grain boundaries crossing the bridges.

I. Introduction

The superconducting quantum interference device (SQUID) is an extremely sensitive magnetic device which can detect faint signals smaller than a tenth of a billionth of the earth field. Because of their ultra high sensitivity, SQUIDs require special measures to eliminate external noises that are typically several orders of magnitude larger than signals to be detected.

*Corresponding author.   Fax : +82 41 860 1327
e-mail : sglee@korea.ac.kr

A magnetically shielded room is a sure solution. However, measurement in unshielded environments is necessary for some applications, such as nondestructive tests and clinical MCG. In such cases a gradiometer type SQUID sensor is an alternative solution because of the immunity to uniform field noises, whose sources are usually located relatively farther from the sensor and thus almost uniform at the sensor position.

The Nb SQUID gradiometer fabricated by the multilayer thin-film process has long been developed [1]. However, a stable and reproducible multiplayer process is not available yet for the high-T_c oxides. Thus, most of the high-T_c junction devices are made from the single superconducting layer. Directly coupled first-order SQUID gradiometer from a single -layer superconductor was developed by Knappe et al. [2]. We developed the 2nd-order SQUID gradiometer from a single layer of superconducting film on a single substrate for the first time [3]. Gradiometers of flip-chip coupling types were also developed. An asymmetric 1st-order SQUID gradiometer with a flip-chip coupling of the pickup coil to the SQUID was developed by Dantsker et al. [4]. The flip-chip coupled 2nd-order high Tc SQUID gradiometer was also developed by Kittel et al. [5]. On the other hand, electronic gradiometers based on electronic subtraction of outputs of magnetometers located at different positions were developed. Koch et al. invented three-SQUID gradiometer with a reference SQUID for baseline field subtraction [6]. Tarvin et al. developed a second-order gradiometer composed of 3 independent sets of SQUID magnetometers [7].

A null balancing in uniform fields is the key issue for the SQUID gradiometer. For flip-chip coupled or electronic gradiometers, the position and orientation of the SQUID sensors are mechanically adjusted for balancing. However, the mechanical adjustment for the 2nd-order gradiometers is very difficult and unstable under vibration or thermal cycling. On the other hand, for single layer gradiometers, balancing is achieved by adjusting one of the device parameters in design. Once the optimum parameters are determined for a particular design, balancing and

stability are guaranteed.

In the previous works we have developed the single-layer 2nd-order SQUID gradiometer [3], and studied detailed balancing of the device [8~9]. In those works, our study on the balancing conditions and noise properties was conducted for short-baseline designs. In this work, we have demonstrated feasibility of the single-layer 2nd-order SQUID gradiometer in magnetocardiography and studied fabrication of 30 mm long baseline gradiometers.

II. Short-baseline 2nd-order SQUID gradiometer

Schematic of the design is shown in Fig. 1. Under a uniform field, the screening currents induced by the flux threading through the side loops flow in opposition direction to that of the center loop in the SQUID loop. When the following condition is satisfied, the flux coupled to the SQUID is zero. That is,

$$2\alpha \frac{A}{L} \cong \alpha_c \frac{A_c}{L_c} + \frac{A_s}{L_s} \qquad (1)$$

where α (α_c) is the portion of SQUID loop in which the screening current induced in one of the side loops (center loop) flow. A (A_c, A_s) and L (L_c, L_s) are the effective area and inductance of the side (center, SQUID) loop, respectively. In this design, $\alpha_c \cong 2\alpha$.
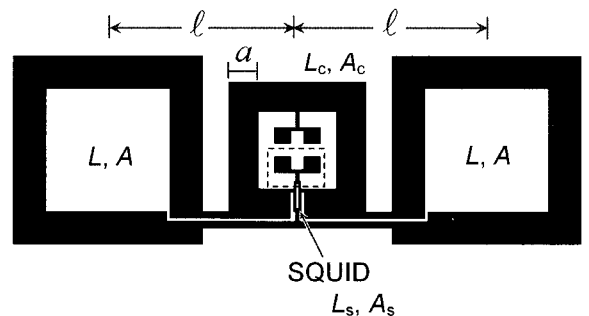

Fig. 1. Schematic of the single-layer 2nd-order SQUID gradiometer. Loop areas are effective values. SQUID area is exaggerated for clarity and the dashed line is the line of the step-edge.

For a balanced gradiometer, the gradient sensitivity is calculated to be

$$\left(\frac{\partial^2 B_z}{\partial x^2}\right)_n \cong \frac{1}{\alpha_c}\frac{\phi_{n,s}}{A_c}\frac{1}{l^2}\frac{L_c}{L_s} \qquad (2)$$

where $\phi_{n,s}$ is the intrinsic SQUID noise. In Eq. (2) the direct-pickup by the SQUID loop was less than 0.01 % in our design and thus neglected.

The gradiometer was 17.6 mm × 6 mm in overall size. The side (center) pickup loop has an inner dimension of 3.6 mm (2.0 mm) with a line width of 1.2 mm (1.134 mm). Effective area and inductance are 21.6 mm^2 (8.54 mm^2) and 8.98 nH (3.60 nH) for the side (center) loop. SQUID inductance is calculated to be 35 pH. Baseline is 5. 8 mm. The balancing conditions were obtained by investigating balancing factor for different values of a around the calculated optimum value. For 5.8 mm baseline device, optimum value was a=1.134 mm with a balancing factor of 6×10^{-4}.

The measured noise spectra are shown in Fig. 2. One can notice that the spectra are 'white' all the way down to 1 Hz for both shielded and unshielded cases, which is in comparison with the usual $1/f$ dependence at low frequencies. Second-order gradient noise is 0.45 pT/cm^2/Hz$^{1/2}$ for the shielded measurement and 0.84 pT/cm^2/Hz$^{1/2}$ for the unshielded case. Equivalent field noises are 150 fT/Hz$^{1/2}$ and 280 fT/Hz$^{1/2}$, respectively. Intrinsic flux noise of the SQUID ($\phi_{n,s}$) is estimated to be 1×10^{-5} ϕ_0/Hz$^{1/2}$ for the shielded and 1.9×10^{-5} ϕ_0/Hz$^{1/2}$ for the unshielded case, which is very low presumably due to the very large common mode rejection of the gradiometer.

The MCG measurements were done in a partially shielded environment with the shielding factor unknown. Lateral MCG signals were recorded with the substrate plane parallel to the chest. Fig. 3 shows 30-time averaged signals, which have clear QRS and T features. The peak height is 24 ~ 30 pT/cm^2, which corresponds to an equivalent field change of 8 ~ 10 pT. The reason that we could measure MCG signals in spite of the short baseline of 5.8 mm is the large common-mode-rejection-ratio, $\delta \approx 10^{-3}$.
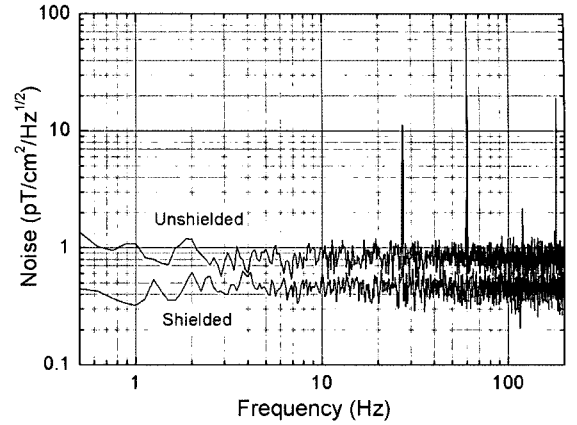

Fig. 2. Noise spectra of the single-layer 2nd-order SQUID gradiometer measured in dc bias. The peak at 27 Hz is the reference signal. Shielded (unshielded) noise is 0.45 pT/cm^2/Hz$^{1/2}$ (0.84 pT/cm^2/Hz$^{1/2}$), which corresponds to the field noise of 150 fT/ Hz$^{1/2}$ (280 fT/Hz$^{1/2}$).
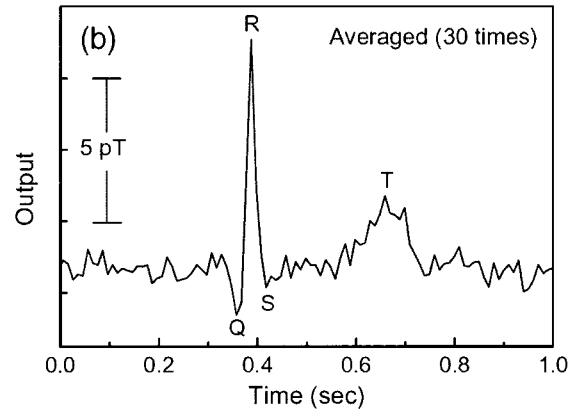

Fig. 3. Measured MCG signals averaged by 30 times.

These results imply feasibility of the newly designed single-layer second-order high-T_c SQUID gradiometer in MCG. However, to get clinically meaningful real time MCG signals a longer-baseline gradiometer is needed.

III. Long-baseline gradiometer

We designed gradiometers with a much longer baseline, 30 mm. The design was based on the same rules as those of the shorter ones. Overall size is 70.2 mm × 10.6 mm with each pickup loop of the outer

dimension of 10 mm × 10 mm. Expected gradient noise is calculated to be 18 fT/cm^2/Hz$^{1/2}$ for an intrinsic SQUID flux noise of 10^{-5} φ$_0$/Hz$^{1/2}$. Unlike the shorter baselines, longer ones are to be made on sapphire substrates, in case of which fabrication of high quality Josephson junctions is the key issue.

We have fabricated submicron bridges by using focused ion beam (FIB). Two types were fabricated, which were variable thickness bridge (VTB) and constant thickness bridge (CTB). Both were patterned from YBCO(300 nm)/Au(50 nm) on a sapphire substrate. VTB is 200 nm thick, 300 nm wide and 30 nm long, and CTB 100 nm wide and 30 nm long with Au layer left on top.

We measured current-voltage (*I-V*) curves and obtained temperature-dependent critical current, $I_c(T)$. Fig. 4 shows *I-V* curves measured at 77 K. One can

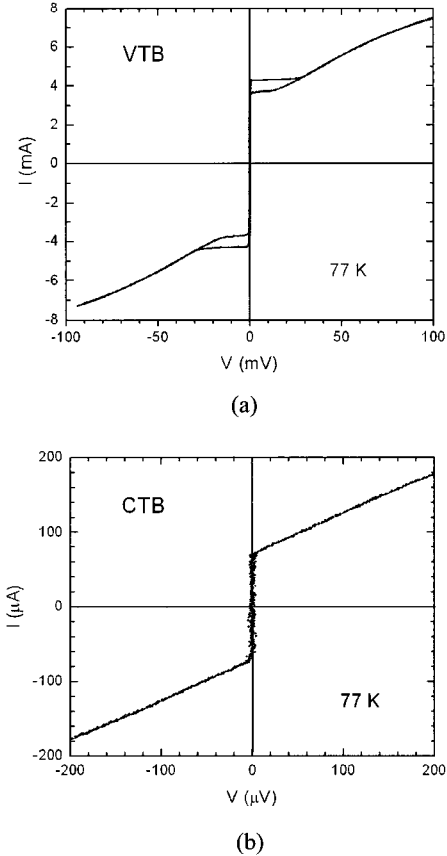clearly notice excess current in CTB. Since the coherence length $\xi_{ab} \sim 1.5$ nm is much shorter than all the bridge dimensions, both VTB and CTB are in the flux flow regime, which explains the excess current. Critical currents are 4.3 mA and 70 µA for VTB and CTB, respectively. Critical current is not proportional to the cross sectional area of the bridge. This non-proportionality is believed due to nonuniform electrical property of the bridge area. We believe that Josephson junction was formed by natural grain boundaries crossing the bridges. $I_c(T)$ data support this conclusion.

Fig. 5 shows temperature-dependent critical current. $I_c(T) \sim (1-T/T_c)^1$ dependence of VTB implies an insulating or at least semiconducting barrier, that is, the bridge behaves as an 'SIS' or SSeS junction. On the other hand, CTB has $I_c(T) \sim (1-T/T_c)^{2.2}$, implying a normal barrier, that is, an 'SNS' junction.

(a)

(b)

Fig. 4. I-V curves measured at 77 K: (a) VTB and (b) CTB.
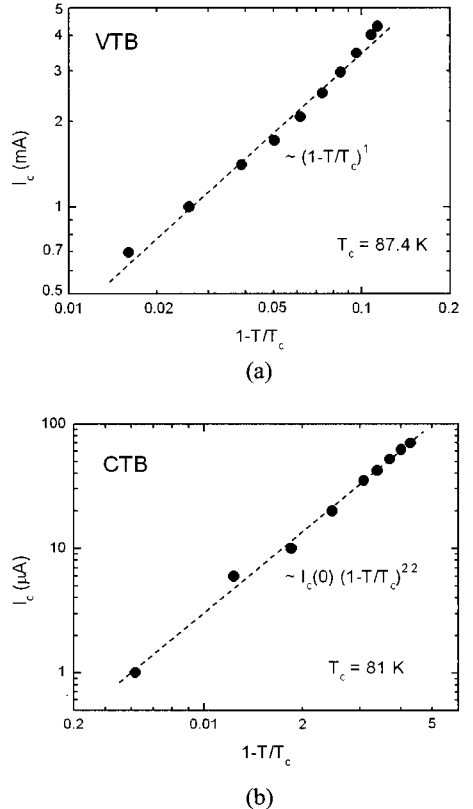

(a)

(b)

Fig. 5. Temperature-dependent critical current and normal state resistance.

Since the superconducting coherence length $\xi_{ab} \sim$ 1.5 nm is much shorter than the width, the length, or thickness of the bridges, they are wide and long bridges. The bridges are in the flux flow regime [10]. In such a case, they behave like a normal-metal-barrier junction. However, our data imply that the metallic is nonmetallic as shown above. We believe that the bridges are crossed by grain boundaries which are naturally abundant in YBCO films. In other words, the bridges are grain boundary (GB) junctions with GB as a nonmetallic barrier. In case of CTB, the bridge is shunted by a 50 nm thick Au layer and thus becomes an 'SNS' weak link. Significant reduction in the slope of the I-V curves, that is, normal state resistance R_N supports our conclusion.

IV. Conclusion

We have studied feasibility of single-layer second-order high-T_c SQUID gradiometers in magnetocardiography. We have measured human MCG signals using a short-baseline (5.8 mm) single-layer second-order YBCO gradiometer in partially shielded environments. Based on the same design rules as the short-baseline devices, we have studied fabrication of 30 mm-long baseline 2nd-order gradiometers. As Josephson elements we made two types of submicron bridges: variable thickness bridge (VTB) and constant thickness bridge (CTB), by using a focused ion beam (FIB) patterning method. Both types were in the flux flow regime. In temperature-dependent critical currents, $I_c(T)$, VTB showed a nonmetallic barrier behavior and CTB a metallic barrier. We believe that those characteristics are ascribed to naturally formed grain boundaries crossing the bridges.

Acknowledgments

References

[1] M. B. Ketchen, W. M. Goubau, J. Clarke, and G. B. Donaldson, "Superconducting thin film gradiometer", J. Appl. Phys., 49, 4111-4116 (1978).

[2] S. Knappe, D. Drung, T. Schurig, H. Koch, M. Klinger, and J. Hinken, "A planar YBa$_2$Cu$_3$O$_7$ gradiometer at 77 K", Cryogenics, 32, 881-884 (1992).

[3] S. G. Lee, Y. Hwang, B. C. Nam, I. S. Kim, and J. T. Kim, "Direct-coupled second-order quantum interference device gradiometer from single layer of high temperature superconductor", Appl. Phys. Lett., 73, 2345-2347 (1998).

[4] E. Dantsker, O. M. Froehlich, S. Tanaka, K. Kouznetzov, J. Clarke, Z. Lu, V. Matijasevic, and K. Char, "High-T$_c$ superconducting gradiometer with a long baseline asymmetric flux transformer", Appl. Phys. Lett., 71, 1712-1714 (1997).

[5] A. Kittel, K. A. Kouznetsov, R. McDermott, B. Oh, and J. Clarke, "High T$_c$ superconducting second-order gradiometer", Appl. Phys. Lett., 73, 2197-2199 (1998).

[6] R. H. Koch, J. Rozen, J. Z. Sun, and W. J. Gallagher, "Three SQUID gradiometer", Appl. Phys. Lett., 63, 403-405 (1993).

[7] Y. Tarvin, Y. Zhang, Y. W. Wolf, and A. I. Braginski, "A second-order SQUID gradiometer operating at 77 K", Supercond. Sci. Technol., 7, 265-268 (1994).

[8] S. G. Lee, Y. Hwang, H. C. Kwon, J. T. Kim, and H. J. Yang, "Improvement of the balance of the single-layer second-order high T$_c$ SQUID gradiometer", Physica C, 372-376, 221-224 (2002).

[9] Y. Hwang, J. R. Ahn, S. G. Lee, J. T. Kim, I. S. Kim, and Y. K. Park, "Balancing of the single-layer second-order high-T$_c$ SQUID gradiometer", IEEE Trans. Appl. Supercond., 11, 1343-1346 (2001).

[10] M. Yu. Kupriyanov, K. K. Likharev, L. A. Maslova, "The Js(φ) relationship, Abrikosov vortices, ans Josephson vortices in variable thickness bridges", LT 14, 4, 104-107 (1975).